Journal of Bioscience and Bioengineering
VOL. 127 No. 5, 641–646, 2019

www.elsevier.com/locate/jbiosc

Glass-based organ-on-a-chip device for restricting small molecular absorption

Hirotada Hirama,[1,*] Taku Satoh,[2] Shinji Sugiura,[2] Kazumi Shin,[2] Reiko Onuki-Nagasaki,[2] Toshiyuki Kanamori,[2] and Tomoya Inoue[1]

Research Center for Ubiquitous MEMS and Micro Engineering, National Institute of Advanced Industrial Science and Technology, 1-2-1 Namiki, Tsukuba, Ibaraki 305-8564, Japan[1] *and Biotechnology Research Institute for Drug Discovery, National Institute of Advanced Industrial Science and Technology, 1-1-1 Higashi, Tsukuba, Ibaraki 305-8565, Japan*[2]

Received 13 July 2018; accepted 26 October 2018
Available online 23 November 2018

The use of organ-on-a-chip (OOC) devices is a promising alternative to existing cell-based assays and animal testing in drug discovery. A rapid prototyping method with polydimethylsiloxane (PDMS) is widely used for developing OOC devices. However, because PDMS tends to absorb small hydrophobic molecules, the loss of test compounds in cell-based assays and increases in background fluorescence during observation often lead to biased results in cell-based assays. To address this issue, we have fabricated a glass-based OOC device and characterized the medium flow and molecular absorption properties in comparison with PDMS-based devices. Consequently, we revealed that the glass device generated a stable medium flow, restricted the absorption of small hydrophobic molecules, and showed enhanced cell adhesiveness. This glass device is expected to be applicable to precise cell-based assays to evaluate small hydrophobic molecules, for which PDMS devices cannot be applied because of their absorption of small hydrophobic molecules.

[**Key words:** Microfluidics; Organ-on-a-chip; Cell-based assay; Glass; Polydimethylsiloxane; Absorption; Cell culture; Flow control]

An organ-on-a-chip (OOC) is a cell culture system with a microscale organ model constructed as a microfluidic device. Such systems are suitable alternatives to enhance the reliability of cell-based assays in drug discovery (1–3). Over the last decade, many types of organs and tissues (e.g., lungs, livers, fat, marrow, and tumors) have been established in OOC (4–8). By combining these organs, a body-on-a-chip has been developed to predict body-level drug responses in multiple-organ systems (9–14). Our group has developed pneumatic pressure-driven OOC systems, which have parallel chambers allowing the simultaneous performance of multiple assays (15–17). Some advantages of our system are pipette-friendly liquid handling, small volume requirement for medium circulation, and simultaneous medium circulation in multiple culture chambers. In most previous works, including our own, OOC devices have been typically fabricated from polydimethylsiloxane (PDMS) because of its unique properties such as transparency, biocompatibility, and ease of microfabrication. However, PDMS-based OOC devices (hereinafter referred to as PDMS devices) can easily absorb small molecules in their polymer network structures (15,18–22). This absorption leads to a loss of available compounds in the culture medium.

To control the absorption of small molecules, various investigations have been conducted. Toepke and Beebe (18) qualitatively studied the absorption of small hydrophobic molecules, while Wang et al. (19) quantitatively studied the same topic. Coatings have been applied to the PDMS surface to prevent molecular absorption, using various materials such as glass and titanium dioxide (20), parylenes (21), and lipophilic materials (22). These coatings have reduced the absorption of small molecules in PDMS. Glass has a higher resistance to small molecular absorption than PDMS; however, absorption with a glass-based OOC device (hereinafter referred to as a glass device) has not yet been investigated. In addition, for applications that require OOC systems, it is crucial to develop a glass device in order to enable the use of reagents that cannot be used for absorption by polymer devices such as PDMS.

In the study described here, we fabricated and characterized a glass device for preventing small molecular absorption in cell-based assays. To fabricate a glass device with dimensions similar to the PDMS device developed in our previous work (17), we redesigned the structure of the microchannels. Using the fabricated glass and PDMS devices, we compared the medium flow behavior, small molecular absorption, and cell adhesiveness. We also performed a lipid staining test in the glass and PDMS devices as an example of a cell-based assay.

MATERIALS AND METHODS

Materials We prepared a 3 μM Nile Red solution in Dulbecco's modified Eagle's medium (DMEM)/F-12 (without phenol red, Thermo Fisher Scientific, Waltham, MA, USA) with 10% fetal bovine serum (FBS) containing 0.1% dimethyl sulfoxide for characterizing small molecular absorption in the glass and PDMS devices. We prepared a 3 μM Nile Red solution in phosphate buffered saline (PBS) containing 3% methanol for lipid staining test. We used poly-L-lysine hydrobromide (PLL) (mol wt 30,000–70,000, Sigma–Aldrich, St. Louis, MO, USA) and collagen (Cellmatrix Type I-C, Nitta Gelatin Inc., Osaka, Japan) for coating the glass and PDMS devices. A human hepatocyte carcinoma cell line, HepG2 cells (RIKEN BioResource Center, Tsukuba, Japan),

* Corresponding author. Tel.: +81 29 861 3065. Fax.: +81 29 861 7225.
E-mail address: h.hirama@aist.go.jp (H. Hirama).

1389-1723/$ – see front matter © 2018, The Society for Biotechnology, Japan. All rights reserved.
https://doi.org/10.1016/j.jbiosc.2018.10.019

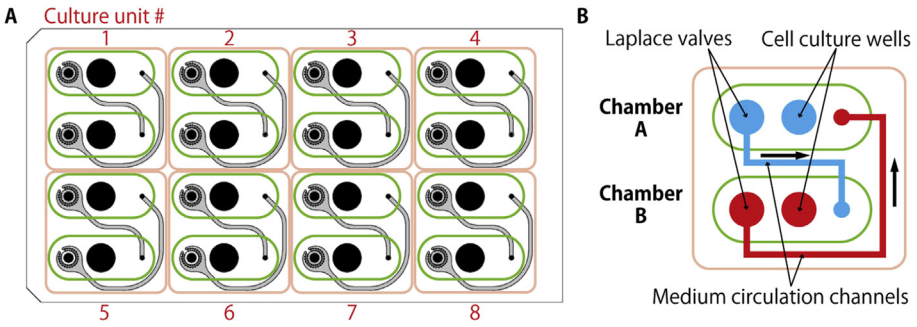

FIG. 1. Structure of the organ-on-a-chip device. (A) Overall view of the device consisting of eight culture units, indicated by pink squares. (B) Schematic of a single culture unit consisting of chambers A and B.

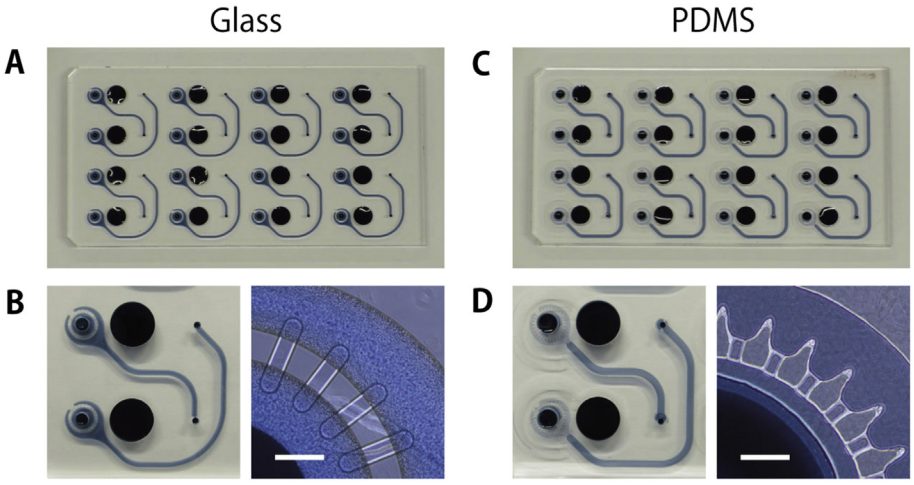

FIG. 2. Organ-on-a-chip devices fabricated from glass (A, B) and PDMS (C, D). (A, C) Overall views of the devices. (B, D) Single culture unit and magnified views of Laplace valves. The scale bars are 500 μm.

was cultured in DMEM (Wako Pure Chemical Industries, Ltd., Osaka, Japan) with 10% FBS and 1% penicillin streptomycin. We prepared a fat-overloading medium containing 0.5 mM oleic acid using oleic acid-albumin from bovine serum (Sigma–Aldrich) in DMEM with 1% penicillin streptomycin and without FBS.

Device design and fabrication We incorporated the device design developed in our previous work (17) to compare the glass and PDMS devices (Fig. 1A). Each device consists of eight culture units, where each culture unit consists of two sets of chambers, Laplace valves, cell culture wells, and medium circulation channels (Fig. 1B). Fig. 2 shows the structure of the glass and PDMS devices used in this study. The structure of the PDMS device was identical to that of the microfluidic plate we used in our previous study (Fig. 2C,D) (17). The structure of the glass device was slightly different from that of the PDMS device (Fig. 2A,B) because of difficulty in the fabrication of the glass device with the same structure with the PDMS device. In this study, the glass devices were fabricated using the following method, which is relatively low in cost, because the fabrication difficulty (which affects fabrication cost) is high for replicating the structure of the PDMS device, which had been fabricated by photolithography and replica molding (i.e., softlithography). The glass device was constructed from two layers of glass plates by wet etching, sandblasting, computer numerical control (CNC) machining, and thermal bonding. Wet etching and sandblasting were performed to engrave deep channels (0.4 mm in depth). CNC machining was performed to engrave cell culture wells on one glass plate. Wet etching was performed to engrave shallow channels as Laplace valves (27 μm in depth) on the other glass plate. After fabricating these structures, thermal bonding was performed to bond the two plates covalently. Technical drawbacks in the fabrication processes and replication of our glass device have been overcome through our previous process development for glass microfabrication (23–28), although harsh chemicals commonly used in wet etching were required. To compare the glass and PDMS devices, we used the PDMS device fabricated in our previous work (17) using soft lithography (29). We used an OOC system composed of a lid, chamber plate, microfluidic plate, and holder to compare the glass and PDMS devices (Fig. S1). In this study, the glass and PDMS devices were used as microfluidic plates, shown in Figs. 2 and S1.

Characterization of flow behavior We used a pneumatic pressure control system (ASTF0401, Engineering System, Japan) to measure the Laplace pressure at which the gas phase breaks into the Laplace valves and to generate medium circulation flow in the glass and PDMS devices, as described in our previous work (17). We estimated the flow rate of the culture medium from the time for medium transfer between chambers A and B. The device was pressurized with 5% CO_2, using a commercial air pump; the gas was supplied from a CO_2 incubator.

Characterization of small molecular absorption To characterize small molecular absorption in the glass and PDMS devices, we introduced 50 μL of the medium with 3 μM Nile Red into the medium circulation channel in the glass and PDMS devices and incubated the devices under light-shielded conditions for 30 min. Exchange with fresh medium was repeated every 30 min, and the medium circulation channels were observed using a fluorescent microscope after 1, 3, 5, and 10 medium introductions.

Characterization of cell adhesiveness To characterize the cell adhesiveness on the glass and PDMS devices, we first treated the cell culture wells in the devices using PLL, coated them with collagen as described in our previous work (17), and compared them with the devices without collagen coating. HepG2 cells were

TABLE 1. Laplace valves in the glass and PDMS devices (n = 3, ±SD).

Device material	Dimensions of the microchannels in the Laplace valves		Laplace pressure (kPa)
	Depth (μm)	Width (μm)	
Glass	27 ± 2	203 ± 1	6.0 ± 0.1
PDMS	27 ± 1	79 ± 1	6.4 ± 0.1

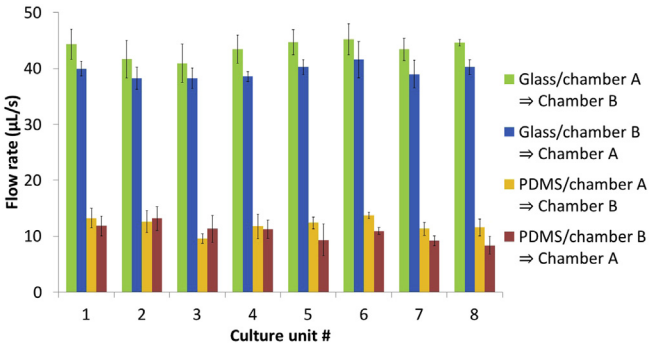

FIG. 3. Flow characteristics. Flow rates in the glass and PDMS device at an applied pressure of 4 kPa (n = 3, mean ± SD).

seeded into the cell culture well at a concentration of 1×10^4 cells/well in the culture medium. Bright-field images were taken 3.5 and 22 h after seeding.

Fat-overloading culture of HepG2 cells and lipid staining To evaluate the effect of small molecular absorption to the glass and PDMS devices during staining experiment, we performed a lipid staining test for HepG2 cells cultured in the fat-overloaded condition, as described in the previous paper (30). Briefly, HepG2 cells were seeded into the cell culture well at the concentration of 1×10^4 cells/well as described in the previous section. Culture medium was exchanged to the fat-overloading medium containing 0.5 mM oleic acid on next day of cell seeding, and the cells were stained after 24 h incubation. The lipid in the fat-overloaded HepG2 cells were stained with 3 μM Nile Red in PBS containing 3% methanol for 30 min and washed with PBS twice; the cells were then observed using fluorescent microscopy.

Microscopy The bright-field and fluorescent images were obtained using cameras (DP25, Olympus, Tokyo, Japan and ORCA-Flash 4.0, Hamamatsu Photonics K.K., Shizuoka, Japan) mounted on inverted microscopes (CKX-41, Olympus, and IX71, Olympus).

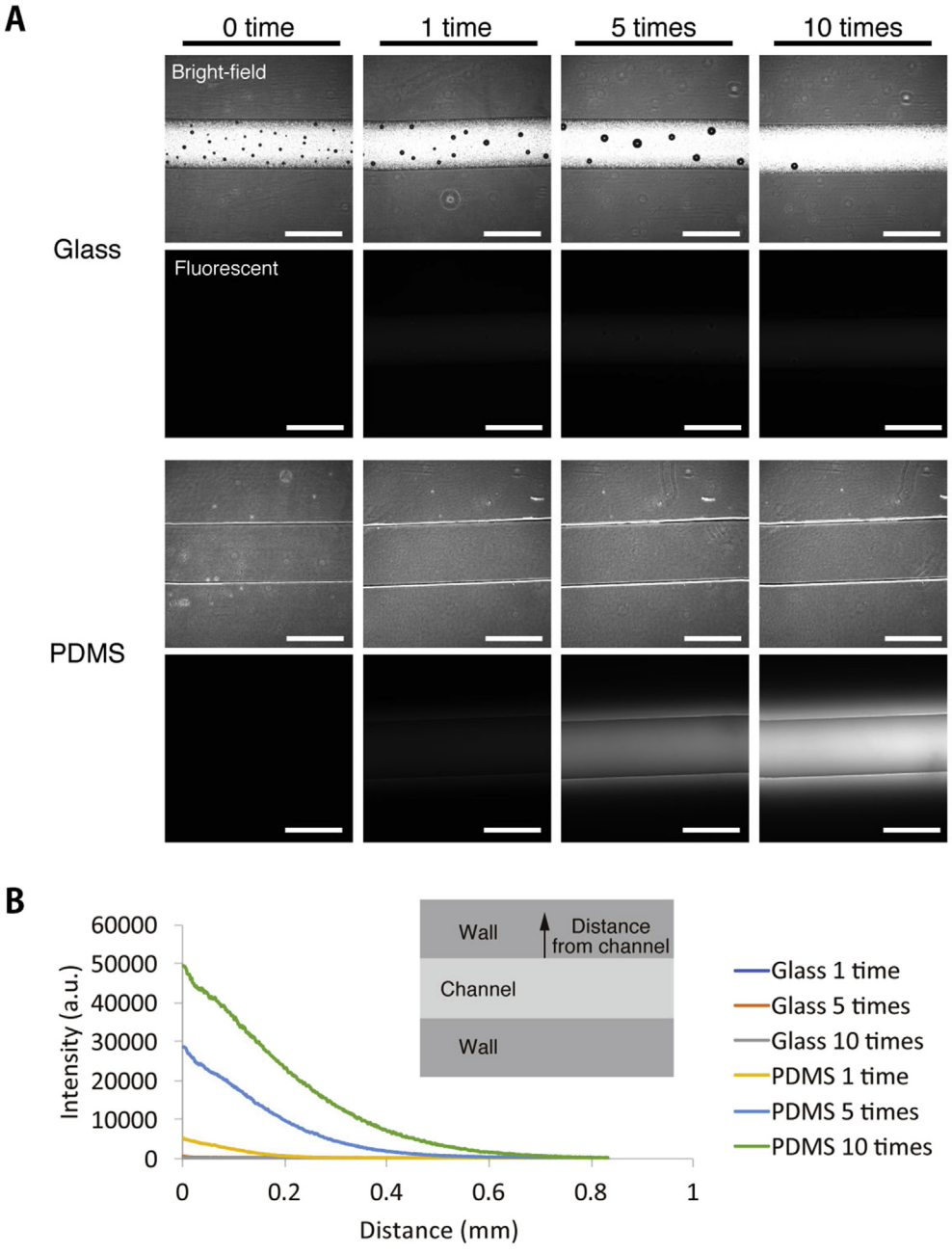

FIG. 4. Comparison of molecular absorption for the glass and PDMS devices. (A) Bright-field and fluorescent images. Fluorescent-dye-added medium was repeatedly introduced to the medium circulation channels and incubated for 30 min. The microscope images were acquired after 0, 1, 5, and 10 introductions of medium. The scale bars are 1 mm. Bright field and fluorescent images were acquired with exposure times of 100 and 500 ms, respectively. (B) Fluorescent intensity in the wall of medium circulation channels.

RESULTS AND DISCUSSION

Fabricated devices and flow behavior We fabricated a glass device with Laplace valves that produce a Laplace pressure similar to that in the PDMS device (Fig. 2 and Table 1). The theoretical Laplace pressure is described by the equation:

$$\Delta P = 2\gamma\left(\frac{1}{w_L}+\frac{1}{h_L}\right) \quad (1)$$

where γ is the interfacial tension and w_L and h_L are the width and height of the microchannels creating the Laplace valve, respectively. In general, the Laplace valves act as passive valves to stop gas flow at the interface between the gas and the liquid at pressures below the Laplace pressure (16,17). The structure of the Laplace valve in the glass device is modified (Fig. 2B,D, and Table 1) from that in the PDMS device to obtain a glass device that produces a Laplace pressure similar to that in the PDMS device used in our previous work (17). The microchannel Laplace valves in the glass device have the same depth as those in the PDMS device but greater width.

We characterized the behavior of the medium flows in the glass and PDMS devices to confirm how the flow rate, an important cell culture condition, changed when different materials were used. The circulation flow of the medium in the devices was generated by sequential applied pressure as described in our previous work (17) (Fig. S1). Here, to measure the flow rates in the glass and PDMS devices, we applied a constant pneumatic pressure of 4 kPa to chambers A and B, repeatedly. Then, the medium flowed from chamber A to chamber B and from chamber B to chamber A, repeatedly. In the glass device, the flow rates from A to B are higher than those from B to A (Fig. 3). This result was consistent with the fluidic resistance difference caused by the longer microchannel from A to B than that from B to A. A similar tendency was observed in the PDMS devices. However, the tendency was different in the different culture units. This difference is most likely because of differences in the deformability of the device (i.e., glass is rigid and PDMS is soft). Because the cross-sectional area of the PDMS device easily varies in response to device deformation, the flow velocity can vary simultaneously.

Molecular absorption and cell adhesion properties Prior to the lipid staining test with the cells in the glass and PDMS devices, we characterized their molecular absorption and cell adhesion properties. We did this by repeating both the introduction of medium with fluorescent dye into the medium circulation channels and the incubation of the devices. The fluorescent intensity of the wall of the medium circulation channel in the PDMS device increases gradually, while no fluorescence is observed in the glass device (Fig. 4). Because of the polymer network structure, PDMS has higher permeability than glass. According to the previous report (18), the molecular absorption for a PDMS-based microchannel decreases the solution concentration in a microchannel to 100 times lower than the original concentration. Therefore, the glass device is more useful than the PDMS device because of its resistance to small molecule absorption. In this experiment, we observe some air bubbles trapped in the microchannels in the glass device (as Fig. 4A). Compared with the PDMS device, air bubbles were frequently formed in the glass device. In general, the untreated glass surface is relatively hydrophobic. This relatively hydrophobic glass surface readily captures air, which forms air bubbles. However, the air bubbles can be easily removed by simply flashing the culture medium several times. Therefore, no interference by air bubbles in the cell culture experiment was observed in this study.

We compared the adhesiveness in the glass and PDMS devices after having cultured HepG2 cells in the culture medium in the culture wells in the glass and PDMS devices. Cells incubated after 22 h are adhered to the surfaces of the glass and PDMS devices, regardless of the presence of surface coatings of collagen (Fig. 5A). Interestingly, in the case of short incubation time (that is, for 3.5 h), the glass device showed immediate cell adhesion, whereas the PDMS device did not (Fig. S2). Under the fat-overloaded condition, under which the medium did not contain FBS, the cells on the collagen-coated PDMS device detached more easily than that on the collagen-coated glass device (Fig. 5B). These results indicate the superior cell adhesion of the glass device compared to the PDMS device under the serum-free condition.

Lipid staining test The effect of the absorption of the fluorescent dye in lipid staining was compared between the glass and PDMS devices. We first confirmed the background fluorescence caused by the absorption of fluorescent dye in the glass and PDMS devices without cells, by incubating the devices with a fluorescent dye, Nile red. As expected, a strong background fluorescence is observed in the PDMS device but not in the glass device (Fig. 6A).

In the next experiment, we incubated the devices with HepG2 cells under the fat-overloaded condition and carried out a lipid staining test. As described in the previous section, the glass device shows higher cell adhesiveness than the PDMS device, even though both devices are coated with PLL and collagen (Fig. 6B). In fluorescent microscopy, the stained lipids are distinguished in the glass device. In contrast, the stained lipids in the PDMS device cannot be distinguished at all, because the fluorescence of cells is buried in the background fluorescence from the culture well. In terms of

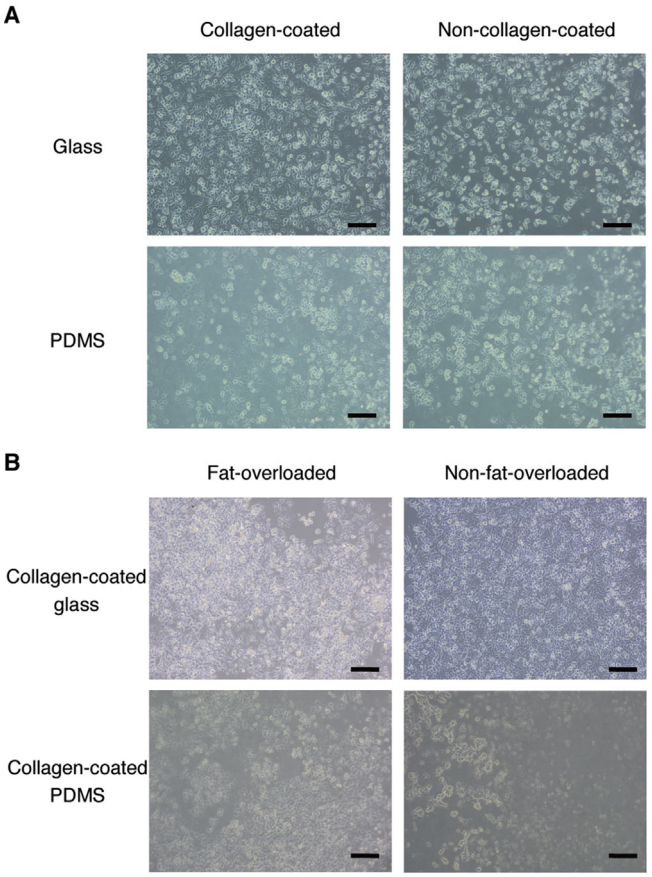

FIG. 5. Comparisons of cell adhesiveness. (A) HepG2 cells cultured on surfaces with and without collagen coating. The cells were incubated in the devices for 22 h after cell seeding. (B) Cells cultured with and without fat-overloading by oleic acid. The cells were incubated in the devices for 24 h after medium change. The scale bars are 200 μm.

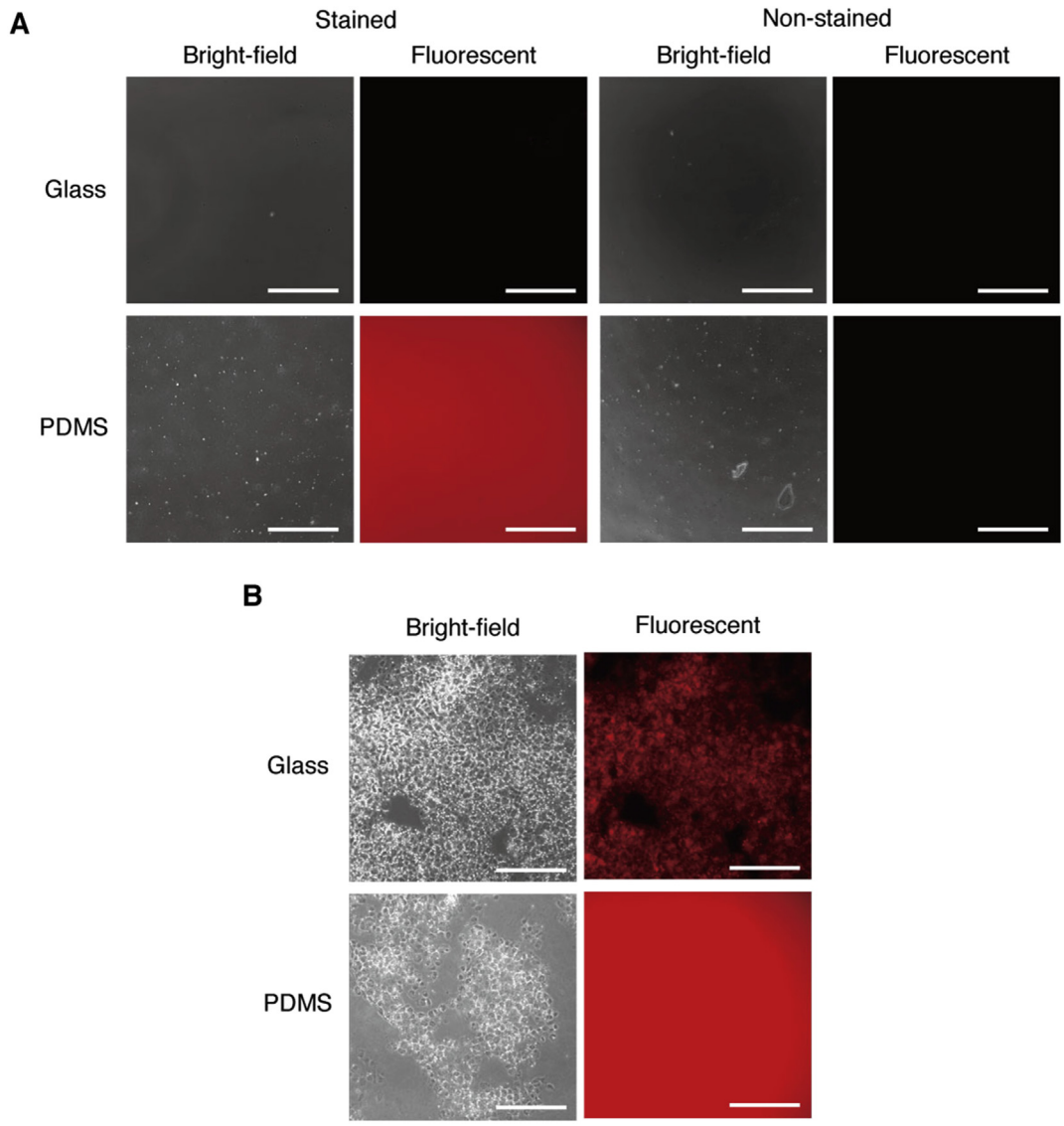

FIG. 6. Lipid staining test with Nile red. (A) Comparisons of background fluorescence in the devices without cells. (B) Lipids stained with a small molecular fluorescent dye. Both the glass and PDMS devices were coated by PLL and collagen in that order. The red color is artificial. The scale bars are 200 μm. The bright field and fluorescent images were taken with exposure times of 100 and 1500 ms, respectively.

fabrication cost, glass devices are approximately 10 times more expensive than PDMS devices based on our discussion regarding fabrication with companies. However, as demonstrated by the above experimental results, the glass device presented here has a high cell adhesiveness and low absorption, and therefore, should be useful in the cell-based assay for analysis of small hydrophobic molecules. This work focused on qualitative studies to investigate cell adhesiveness and small molecular absorption in a glass device. In a future work, a quantitative study with a glass device should be performed, because the results could assist in determining how much the molecules are absorbed or not. We expect that the glass-based OOC device may be widely applicable to cell-based assays to evaluate rare and valuable small-molecule drug candidates.

Supplementary data to this article can be found online at https://doi.org/10.1016/j.jbiosc.2018.10.019.

ACKNOWLEDGMENTS

We thank TECNISCO Ltd. for assistance in the design of the glass device. H.H., S.S., and T.K. proposed the concept. T.S. and S.S. designed the microfluidic devices. S.S., K.S., and R.N. designed the cell culture experiment. K.S. performed the flow characterization. K.S. and R.N. performed the absorption study and cell culture experiment. T.K. and T.I. supervised the study. All authors reviewed and provided comments on the manuscript.

References

1. **Bhatia, S. N. and Ingber, D. E.:** Microfluidic organs-on-chips, Nat. Biotechnol., **32**, 760–772 (2014).
2. **Shuler, M. L.:** Organ-, body- and disease-on-a-chip systems, Lab Chip, **17**, 2345–2346 (2017).
3. **Esch, E. W., Bahinski, A., and Huh, D.:** Organs-on-chips at the frontiers of drug discovery, Nat. Rev. Drug Discov., **14**, 248–260 (2015).
4. **Viravaidya, K. and Shuler, M. L.:** Incorporation of 3T3-L1 cells to Mimic bioaccumulation in a microscale cell culture analog device for toxicity studies, Biotechnol. Prog., **20**, 590–597 (2004).
5. **Sin, A., Chin, K. C., Jamil, M. F., Kostov, Y., Rao, G., and Shuler, M. L.:** The design and fabrication of Three-chamber microscale cell culture analog devices with integrated dissolved oxygen sensors, Biotechnol. Prog., **20**, 338–345 (2004).

6. **Mahler, G. J., Esch, M. B., Glahn, R. P., and Shuler, M. L.:** Characterization of a gastrointestinal tract microscale cell culture analog used to predict drug toxicity, Biotechnol. Bioeng., **104**, 193–205 (2009).
7. **Tatosian, D. A. and Shuler, M. L.:** A novel system for evaluation of drug mixtures for potential efficacy in treating multidrug resistant cancers, Biotechnol. Bioeng., **103**, 187–198 (2009).
8. **Sung, J. H. and Shuler, M. L.:** A micro cell culture analog (microCCA) with 3-D hydrogel culture of multiple cell lines to assess metabolism-dependent cytotoxicity of anti-cancer drugs, Lab Chip, **9**, 1385–1394 (2009).
9. **Lee, H. and Cho, D.-W.:** One-step fabrication of an organ-on-a-chip with spatial heterogeneity using a 3D bioprinting technology, Lab Chip, **16**, 2618–2625 (2016).
10. **Sung, J. H., Esch, M. B., Prot, J.-M., Long, C. J., Smith, A., Hickman, J. J., and Shuler, M. L.:** Microfabricated mammalian organ systems and their integration into models of whole animals and humans, Lab Chip, **13**, 1201–1212 (2013).
11. **Imura, Y., Sato, K., and Yoshimura, E.:** Micro Total bioassay system for ingested substances: assessment of intestinal absorption, hepatic metabolism, and bioactivity, Anal. Chem., **82**, 9983–9988 (2010).
12. **Imura, Y., Yoshimura, E., and Sato, K.:** Micro Total bioassay system for oral drugs: evaluation of gastrointestinal degradation, intestinal absorption, hepatic metabolism, and bioactivity, Anal. Sci., **28**, 197–199 (2012).
13. **Imura, Y., Yoshimura, E., and Sato, K.:** Microcirculation system with a dialysis part for bioassays evaluating anticancer activity and retention, Anal. Chem., **85**, 1683–1688 (2013).
14. **Wikswo, J. P., Curtis, E. L., Eagleton, Z. E., Evans, B. C., Kole, A., Hofmeister, L. H., and Matloff, W. J.:** Scaling and systems biology for integrating multiple organs-on-a-chip, Lab Chip, **13**, 3496–3511 (2013).
15. **Sugiura, S., Hattori, K., and Kanamori, T.:** Microfluidic serial dilution cell-based assay for analyzing drug dose response over a wide concentration range, Anal. Chem., **82**, 8278–8282 (2010).
16. **Satoh, T., Narazaki, G., Sugita, R., Kobayashi, H., Sugiura, S., and Kanamori, T.:** A pneumatic pressure-driven multi-throughput microfluidic circulation culture system, Lab Chip, **16**, 2339–2348 (2016).
17. **Satoh, T., Sugiura, S., Shin, K., Onuki-Nagasaki, R., Ishida, S., Kikuchi, K., Kakiki, M., and Kanamori, T.:** A multi-throughput multi-organ-on-a-chip system on a plate formatted pneumatic pressure-driven medium circulation platform, Lab Chip, **18**, 115–125 (2018).
18. **Toepke, M. W. and Beebe, D. J.:** PDMS absorption of small molecules and consequences in microfluidic applications, Lab Chip, **6**, 1484–1486 (2006).
19. **Wang, J. D., Douville, N. J., Takayama, S., and ElSayed, M.:** Quantitative analysis of molecular absorption into PDMS microfluidic channels, Ann. Biomed. Eng., **40**, 1862–1873 (2012).
20. **Gomez-Sjoberg, R., Leyrat, A. A., Houseman, B. T., Shokat, K., and Quake, S. R.:** Biocompatibility and reduced drug absorption of Sol–Gel-treated poly(dimethyl siloxane) for microfluidic cell culture applications, Anal. Chem., **82**, 8954–8960 (2010).
21. **Sasaki, H., Onoe, H., Osaki, T., Kawano, R., and Takeuchi, S.:** Parylene-coating in PDMS microfluidic channels prevents the absorption of fluorescent dyes, Sensors Actuators B Chem., **150**, 478–482 (2010).
22. **van Meer, B. J., de Vries, H., Firth, K. S. A., van Weerd, J., Tertoolen, L. G. J., Karperien, H. B. J., Jonkheijm, P., Denning, C., IJzerman, A. P., and Mummery, C. L.:** Small molecule absorption by PDMS in the context of drug response bioassays, Biochem. Biophys. Res. Commun., **482**, 323–328 (2017).
23. **Inoue, T., Schmidt, M. A., and Jensen, K. F.:** Microfabricated multiphase reactors for the direct synthesis of hydrogen peroxide from hydrogen and oxygen, Ind. Eng. Chem. Res., **46**, 1153–1160 (2007).
24. **Inoue, T., Ohtaki, K., Adachi, J., Lu, M., and Murakami, S.:** Direct synthesis of hydrogen peroxide using glass fabricated microreactor – multichannel operation and catalyst comparison, Catal. Today, **248**, 169–176 (2015).
25. **Inoue, T., Ohtaki, K., Kikutani, Y., Sato, K., Nishioka, M., Hamakawa, S., Mawatari, K., Mizukami, F., and Kitamori, T.:** The direct synthesis of hydrogen peroxide (ca. 5 wt %) from hydrogen and oxygen by microreactor technology, Chem. Lett., **38**, 820–821 (2009).
26. **Inoue, T., Kikutani, Y., Hamakawa, S., Mawatari, K., Mizukami, F., and Kitamori, T.:** Reactor design optimization for direct synthesis of hydrogen peroxide, Chem. Eng. J., **160**, 909–914 (2010).
27. **Inoue, T., Adachi, J., Ohtaki, K., Lu, M., Murakami, S., Sun, X., and Wang, D. F.:** Direct hydrogen peroxide synthesis using glass microfabricated reactor – Paralleled packed bed operation, Chem. Eng. J., **278**, 517–526 (2015).
28. **Hirama, H., Yoshioka, H., Matsumoto, Y., Arvada, T., Hori, Y., Ohtaki, K., Lu, M., and Inoue, T.:** Design, fabrication, and performance of an optimized flow reactor with parallel micropacked beds, Ind. Eng. Chem. Res., **56**, 14200–14206 (2017).
29. **Xia, Y. N. and Whitesides, G. M.:** Soft lithography, Annu. Rev. Mater. Sci., **28**, 153–184 (1998).
30. **Gomez-Lechon, M. J., Donato, M. T., Martinez-Romero, A., Jimenez, N., Castell, J. V., and O'Connor, J. E.:** A human hepatocellular in vitro model to investigate steatosis, Chem. Biol. Interact., **165**, 106–116 (2007).